Live Imaging of Nitric Oxide Dynamics Reveals Cell Type–Specific NO Signaling in Air–Liquid Interface Cultures of Human Sinonasal Epithelial Cells

Sakura Hirokane , Keiichiro Kiyohara , Sachio Takeno * , Tsuyoshi Sugimoto , Tomohiro Kawasumi , Yukako Okamoto , Rikuto Fujita , Chie Ishikawa , Yuichiro Horibe , Takashi Ishino , Takao Hamamoto , Tsutomu Ueda

Posted Date: 18 May 2026

doi: 10.20944/preprints202605.1116.v1

Keywords: paranasal sinus; chronic rhinosinusitis; nasal polyps; ciliated cells; nitric oxide; nitric oxide synthase; air–liquid interface culture; mucociliary clearance

 doi:10.20944/preprints202605.1116.v1

Article

Live Imaging of Nitric Oxide Dynamics Reveals Cell Type–Specific NO Signaling in Air–Liquid Interface Cultures of Human Sinonasal Epithelial Cells

Sakura Hirokane, Keiichiro Kiyohara, Sachio Takeno *, Tsuyoshi Sugimoto, Tomohiro Kawasumi, Yukako Okamoto, Rikuto Fujita, Chie Ishikawa, Yuichiro Horibe, Takashi Ishino, Takao Hamamoto and Tsutomu Ueda

Department of Otorhinolaryngology, Head and Neck Surgery, Graduate School of Biomedical Sciences, Hiroshima University, Hiroshima 734-8551, Japan

* Correspondence: takeno@hiroshima-u.ac.jp; Tel.: +81-82-257-5252; Fax: +81-82-257-5254

Abstract

Background/Objectives: Chronic rhinosinusitis with nasal polyps (CRSwNP) is characterized by epithelial remodeling, impaired mucociliary clearance, and altered nitric oxide (NO) metabolism. However, the cell type–specific mechanisms of NO production and the functional roles of nitric oxide synthase (NOS) isoforms in sinonasal epithelial cells remain unclear. This study investigated NO production dynamics in air–liquid interface (ALI) cultures of human sinonasal epithelial cells. **Methods:** Human sinonasal epithelial cells were differentiated under ALI conditions. Expression of inducible NOS (iNOS) and endothelial NOS (eNOS) was analyzed by quantitative RT-PCR. Intracellular NO production was evaluated using the NO-sensitive fluorescent probe DAF-FM combined with laser scanning confocal microscopy. Cell type–specific NO production was examined in ciliated and non-ciliated epithelial cells using the NOS inhibitors L-NAME and 1400W. **Results:** CRSwNP tissues demonstrated significantly increased iNOS expression and elevated iNOS/eNOS ratios compared with controls, whereas eNOS expression showed no significant difference. ALI cultures successfully reproduced differentiated sinonasal epithelium containing ciliated and basal cells. DAF-FM fluorescence revealed significantly greater NO production in ciliated epithelial cells than in non-ciliated cells. Non-selective NOS inhibition by L-NAME markedly suppressed NO production in both cell types, whereas selective iNOS inhibition by 1400W reduced but did not abolish NO production in ciliated cells. **Conclusions:** NO production mechanisms differ according to sinonasal epithelial cell subtype. Ciliated epithelial cells maintain both eNOS- and iNOS-dependent NO production, whereas non-ciliated cells predominantly rely on iNOS-derived NO. Dysregulated spatial NO signaling associated with ciliated cell loss may contribute to epithelial dysfunction and chronic inflammation in CRSwNP.

Keywords: paranasal sinus; chronic rhinosinusitis; nasal polyps; ciliated cells; nitric oxide; nitric oxide synthase; air–liquid interface culture; mucociliary clearance

1. Introduction

Chronic rhinosinusitis (CRS) is a chronic inflammatory disease of the nasal cavity and paranasal sinuses characterized by persistent symptoms such as nasal obstruction, rhinorrhea, and olfactory dysfunction. CRS is increasingly recognized not as a single disease entity, but as a heterogeneous group of disorders with distinct inflammatory profiles and molecular mechanisms [1–4]. In particular, the importance of endotype-based classification centered on type 2 inflammation has been emphasized in chronic rhinosinusitis with nasal polyps (CRSwNP) [5–7].

Impaired mucociliary clearance is considered a key pathological feature of CRS. Airway cilia play an essential role in host defense by removing inhaled pathogens and foreign particles through

 doi:10.20944/preprints202605.1116.v1

coordinated mucociliary transport. However, persistent inflammation and infection in CRS disrupt ciliary function, leading to impaired mucociliary clearance and perpetuation of chronic inflammation. Recent advances in single-cell RNA sequencing analyses have revealed a reduction in ciliated epithelial cells, epithelial differentiation abnormalities, and metabolic dysregulation in CRSwNP, highlighting the importance of epithelial remodeling in disease pathogenesis [8,9].

Nitric oxide (NO) is an important signaling molecule in the airway epithelium that exerts antimicrobial activity and enhances ciliary motility, both of which are essential for maintaining mucociliary clearance [10–13]. NO is synthesized primarily by nitric oxide synthase (NOS), and two NOS isoforms, endothelial NOS (eNOS) and inducible NOS (iNOS), play major roles in the airway epithelium [14]. Under physiological conditions, low concentrations of NO derived from eNOS contribute to the regulation of ciliary motility. In contrast, sustained high-output NO production by iNOS may contribute to oxidative stress and tissue injury under inflammatory conditions. Furthermore, eNOS has been shown to be specifically expressed in ciliated epithelial cells of the respiratory tract and to regulate ciliary beating through the NO–cGMP signaling pathway [15]. These findings suggest that epithelial-derived NO plays a central role in maintaining mucociliary transport.

Interestingly, although decreased nasal nitric oxide (nNO) levels have been consistently reported in patients with CRSwNP, increased iNOS expression has also been observed at the tissue level [16,17]. These findings suggest that NO abnormalities in CRS may not simply reflect reduced NO production, but rather qualitative alterations in NO signaling associated with changes in the balance of NOS isoforms.

However, the mechanisms regulating NO production according to epithelial differentiation status and epithelial cell subtype remain poorly understood. Although reduced nNO levels and increased iNOS expression have been described in CRSwNP, the cell type–specific functional roles of NOS isoforms and their contribution to NO production have not been fully elucidated. In particular, little is known regarding differences in NO signaling between ciliated and non-ciliated epithelial cells.

Therefore, in the present study, we established an air–liquid interface (ALI) culture model using human sinonasal epithelial cells and investigated differences in NO production capacity and the functional involvement of NOS isoforms between ciliated and non-ciliated epithelial cells. In addition, by using NOS inhibitors, we aimed to clarify cell type–specific mechanisms of NO production and to explore the pathophysiological significance of altered NO signaling in CRSwNP.

To visualize intracellular NO production, fluorescence imaging using the NO-sensitive fluorescent probe DAF-FM was performed, and fluorescence intensity was quantitatively analyzed to compare NO production capacity between epithelial cell subtypes [18]. Using this approach combined with immunohistochemistry and laser scanning confocal microscopy (LSCM), we identified heterogeneity in NO production and bioavailability among epithelial cell subtypes, including basal and ciliated cells, providing new insights into the spatial regulation of NO signaling within the sinonasal epithelium.

2. Materials and Methods

2.1. Study Design and Tissue Samples

All procedures in this study complied with the ethical standards outlined in the Helsinki Declaration. The study protocol was approved by the Institutional Review Board of Hiroshima University School of Medicine (approval no. Hi-136-4; approval date: 2 November 2022). Written informed consent was obtained from all participants prior to inclusion.

We enrolled patients with chronic rhinosinusitis with nasal polyps (CRSwNP) and control subjects who underwent endoscopic endonasal sinus surgery between April 2024 and August 2025. Tissue samples were collected from the ethmoid sinus and nasal polyps during surgery. The diagnosis of CRS was based on patients' history, clinical symptoms, nasal endoscopic findings, and computed tomography (CT) images [1]. Patients who had previously undergone sinus surgery were excluded. None of the participants had received systemic or topical corticosteroids for ≥4 weeks prior

 doi:10.20944/preprints202605.1116.v1

to surgery. Allergic rhinitis (AR) was diagnosed according to clinical history, nasal symptoms, positive nasal eosinophil findings, and positive allergen-specific IgE antibodies against common airborne allergens. Control subjects were patients without sinus infection who underwent endonasal surgery and had normal paranasal sinus mucosa with normal radiological findings.

2.2. Air-Liquid Interface (ALI) Culture

Human sinonasal epithelial cells (HSNECs) were isolated by enzymatic dissociation in minimal essential medium (MEM; MilliporeSigma, St. Louis, MO, USA) containing 1.0 mg/mL protease (MilliporeSigma) and 0.01 mg/mL DNase (MilliporeSigma) for 24 h at 4 °C, followed by washing with bronchial epithelial growth medium (BEGM). The epithelial cells were collected by centrifugation using a cell scraper and seeded on tissue culture dishes coated with type I collagen (IWAKI, Shizuoka, Japan) in BEGM supplemented with 100 U/mL penicillin and 100 μg/mL streptomycin. The cultures were maintained at 37 °C in a humidified atmosphere with 5% CO_2. The culture medium was replaced every 2–3 days. Primary sinonasal epithelial cells were cultured for 6–7 days until reaching 80% confluence (1.7–4.0 × 10^6 cells/dish).

Passage-2 HSNECs (1.5 × 10^5 cells/well) were seeded for ALI culture in 0.5 mL of medium on Transwell clear culture inserts (12 mm diameter, 0.4 μm pore size; Costar, Corning Inc., Corning, NY, USA), as previously described [19]. Initially, cells were cultured under submerged conditions in BEGM with supplements for 5–7 days. Once confluence was achieved, the apical medium was removed to establish an ALI. Thereafter, only the basal medium was replenished every 2–3 days.

2.3. Scanning Electron Microscopy (SEM)

ALI culture specimens were fixed in 2.5% glutaraldehyde and 2% paraformaldehyde in 0.1 M phosphate buffer (pH 7.4). After fixation, samples were rinsed three times in distilled water, post-fixed in 2% osmium tetroxide for 2 h, and dehydrated through a graded ethanol series (50%, 70%, 80%, 90%, 95%, and 100%). Specimens were then immersed in tert-butanol for 1.5 h and dried using a t-butanol freeze-drying device (VFD-21S; Vacuum Device Inc., Ibaraki, Japan). The dried samples were sputter-coated with osmium (Neoc-ST; Meiwa Forsys, Tokyo, Japan) and examined using a JSM-7800F scanning electron microscope (JEOL Ltd., Tokyo, Japan). Cell types were identified, and their relative proportions were calculated as mean percent surface area. Ciliary synchronization, defined as the percentage of cilia "in phase" with the metachronal pattern, was evaluated after whole-surface scanning as described elsewhere [20].

2.4. Quantitative RT-PCR Analysis

Samples were preserved in RNAlater™ (Thermo Fisher Scientific, Waltham, MA, USA). Quantitative RT-PCR was performed using an ABI Prism 7300 system (Applied Biosystems, Foster City, CA, USA) as previously described [21]. Total RNA was extracted using RNeasy Mini Kits (Qiagen, Valencia, CA, USA) and reverse-transcribed to cDNA using a High-Capacity RNA-to-cDNA Kit (Applied Biosystems).

Gene expression was quantified using TaqMan Gene Expression Assays (Thermo Fisher Scientific) for iNOS (NOS2) (Hs01075529_m1), eNOS (NOS3) (Hs01574665_m1), and BCAM (Hs00170663_m1). GAPDH (Hs02786624_g1) served as an internal control. Relative expression was calculated using the comparative Ct ($2^{-}\Delta\Delta Ct$) method and expressed as the ratio of target gene to GAPDH expression.

2.5. Immunofluorescence Microscopy

Primary antibodies included anti-human Arl13B rabbit polyclonal antibody (#17711-1-AP; Proteintech, Rosemont, IL, USA; 1:500), anti-BCAM (basal cell adhesion molecule) mouse monoclonal antibody (#sc-365191; Santa Cruz Biotechnology, Dallas, TX, USA; 1:100) and anti-human acetylated α-tubulin mouse monoclonal antibody (#SC-23950; Santa Cruz Biotechnology, Dallas, TX, USA;

 doi:10.20944/preprints202605.1116.v1

1:500). ALI cultures were fixed in 4% paraformaldehyde for 20 min at room temperature. Non-specific binding was blocked by incubation with 10% goat serum for 1 h. Cultures were incubated overnight at 4 °C with the primary antibodies, followed by the appropriate secondary antibodies—anti-mouse goat IgG Alexa Fluor® 555 (#A32727; Invitrogen, Carlsbad, CA; 1:100) and anti-rabbit IgG goat Alexa Fluor® 488 (#A32731; Invitrogen; 1:100). Nuclei were counterstained with DAPI (#71-03-00; KPL, Gaithersburg, MD, USA) in PBST containing 0.01% sodium azide for 1 h. After washing with PBS, samples were mounted in VECTASHIELD Antifade Mounting Medium (#H-1000-10; Vector Laboratories, CA, USA) and imaged using a laser scanning confocal microscope (Stellaris 5; Leica, Germany). IgG1 isotype controls confirmed the absence of non-specific staining.

2.6. Live Cell Imaging of Nitric Oxide (NO) Production

Live-cell imaging of NO production was performed as described previously [22–25]. ALI cultures were incubated on the apical side with 10 μM DAF-FM diacetate (#SK1004-01; Goryo Chemical, Japan) in HBSS for 30 min. DAF-FM has optimal excitation and emission wavelengths of 495 and 515 nm, respectively. The incubation time and concentration of DAF-FM were determined based on preliminary experiments and published data [26]. To stimulate NO production, L-arginine was added to the solution at a final concentration of 0.5 mM.

Differential interference contrast (DIC) microscopy was used simultaneously to identify ciliated cell-rich regions in ALI cultures. To confirm NO production by specific cell types, double-label immunofluorescence for acetylated tubulin was performed on DAF-FM–loaded samples fixed in 4% paraformaldehyde in 0.1 M phosphate buffer (PB) for 30 min at 20 °C. To assess the contribution of each NOS isoform to NO production, ALI cells were treated during DAF-FM incubation with either 0.5 mM NG-nitro-L-arginine methyl ester (L-NAME), a non-specific NOS inhibitor, or 100 μM 1400W, a selective iNOS inhibitor.

2.7. Quantitative Image Analysis

Fluorescence intensities of DAPI, DAF-FM, and acetylated tubulin were quantified using ImageJ software (NIH, Bethesda, MD, USA) as described previously [27]. Regions of interest (ROIs) were defined using the ROI Manager to match acetylated tubulin-positive cells at the apical surface, standardized to 1924 pixels per ROI. Laser scanning confocal images were split by channel, converted to 16-bit grayscale, and analyzed for mean fluorescence intensity. For each ALI culture, 50 fields of view were analyzed.

2.8. Statistical Analysis

Statistical analyses were performed using GraphPad Prism software [version 8.0, San Diego, CA, USA]. Multiple groups were compared by one-way or two-way analysis of variance with Dunn's and Geisser–Greenhouse correction, respectively; two groups were compared using the Mann–Whitney test with a Welch post-test correction. Data distribution was assessed using the Shapiro–Wilk test. $P < 0.05$ was considered significant.

All procedures in this study complied with the ethical standards expressed in the Helsinki Declaration. The study protocol was approved by the Institutional Review Board of Hiroshima University School of Medicine (approval no. E2014-9136; approval date: 2 November 2022). Written informed consent was obtained from all patients prior to their participation.

3. Results

3.1. Comparison of NOS Isoform mRNA Expression in CRSwNP Patients

The demographic and clinical characteristics of the study population are summarized in Table 1. No significant differences were observed between the control group (n = 20) and the CRSwNP group (n = 20) with respect to age, sex, body mass index (BMI), prevalence of allergic rhinitis and

 doi:10.20944/preprints202605.1116.v1

bronchial asthma, or peripheral blood eosinophil counts. In contrast, tissue eosinophil counts were significantly higher in the CRSwNP group than in the control group ($p < 0.001$). In addition, CT scores were significantly elevated in the CRSwNP group, reflecting increased disease severity (Table 1).

Table 1. Background and baseline characteristics of the study population.

	Controls	CRSwNP
n (male/female)	20 (10/10)	20 (10/10)
Age (mean ± SD)	47.4 ± 13.6	54 ± 11.1
BMI, kg/mm^2 (mean ± SD)	23.9 ± 4.4	22.1 ± 2.5
Allergic rhinitis (%)	11 (55%)	14 (70%)
Bronchial asthma (%)	1 (5%)	4 (20%)
CT score (mean ± SD)	NA	12.5 ± 4.8
Blood eosinophils (%) (median, range)	2.6 (0.6–8.8)	4.45 (0.7–13.9)
Tissue eosinophils (cells/HPF) (median, range)	3 (0–25)	74.2 (0.0–333.3) ***

Data are shown as mean ± standard deviation (SD), median (range), or number (%). *** $p < 0.001$ vs. the control group. CRSwNP, chronic rhinosinusitis with nasal polyp; BMI, body mass index; HPF, high power field (x400); CT, computed tomography.

mRNA expression levels of NOS isoforms (iNOS and eNOS) in ethmoid sinus mucosa were analyzed by RT-PCR (Figure 1). iNOS expression was significantly increased in the CRSwNP group compared with the control group, whereas no significant difference in eNOS expression was observed between the two groups. Furthermore, the iNOS/eNOS ratio was significantly elevated in the CRSwNP group, suggesting qualitative alterations in NO signaling under inflammatory conditions.

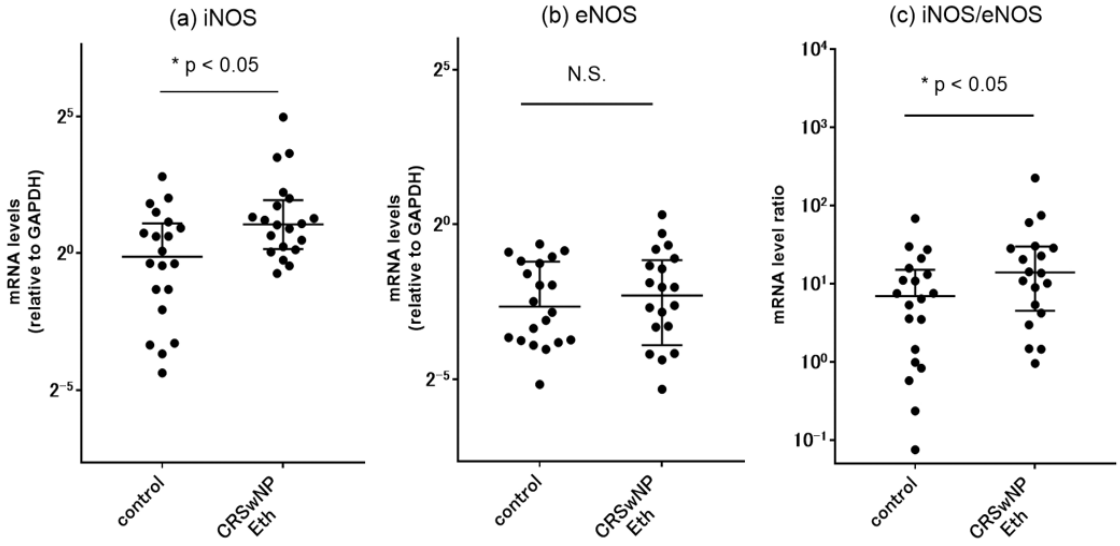

Figure 1. Comparison of the mRNA expressions in ethmoid sinus mucosa from the controls (n=20) and CRSwNP patients (n=20) as detected by RT-PCR. The (**a**) iNOS and (**b**) eNOS mRNA levels were quantitatively normalized against GAPDH levels. (**c**) Comparison of the mRNA expression ratios of iNOS to eNOS for each subject in the control and CRSwNP groups. Center lines: median values. Error bars: interquartile ranges. N.S., not significant; CRS, chronic rhinosinusitis; Eth, ethmoid; NP, nasal polyps.

 doi:10.20944/preprints202605.1116.v1

3.2. Phenotypic Identification and Morphological Evaluation of ALI-Cultured Cells

To investigate the differentiation process toward ciliated epithelial cells and their NO-producing capacity in vitro, primary sinonasal epithelial cells were isolated from surgical specimens obtained during sinus surgery and expanded in basal cell growth medium prior to differentiation under air–liquid interface (ALI) conditions. After enzymatic dissociation, cells were seeded at high density onto permeable Transwell filters, and the apical medium was removed on the following day. This procedure exposed the luminal surface of epithelial cells to air and induced differentiation from basal cells into ciliated epithelial cells.

To determine whether the sinonasal epithelial phenotype was preserved during ALI culture, surface morphology and protein/gene expression profiles were evaluated. Scanning electron microscopy (SEM) demonstrated epithelial cells arranged in a cobblestone-like pattern with characteristic microvilli typical of respiratory epithelium (Figure 2). Low-magnification images obtained after 4 weeks of ALI culture showed that approximately half of the epithelial surface was covered by ciliated cells. High-magnification images revealed clustered ciliated cells; however, ciliary orientation appeared disorganized, and coordinated metachronal waves observed in vivo were not clearly reproduced. The proportion of ciliated cells reached a maximum at 3–4 weeks after ALI induction. These findings were consistent with a previous report demonstrating that human sinonasal epithelial cells differentiate into respiratory epithelium under ALI conditions and require approximately 14 days for mature ciliogenesis [28].

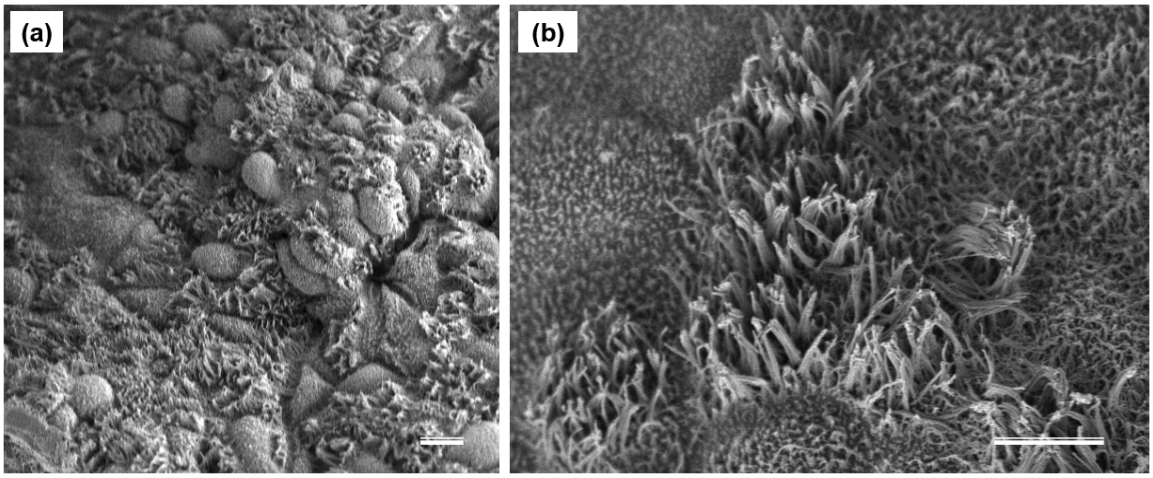

Figure 2. Representative SEM photomicrographs showing surface morphology and cell types of ALI cultured cells. (**a**) The SEM image at lower magnification on day 14 of culture shows approximately half of the surface epithelium is covered with ciliated cells. (**b**) The SEM image at higher magnification shows a cluster of ciliated cells. In these cells, ciliary synchronization as revealed by the typical metachronal pattern is relatively poor with random orientations. Scale bars: 10 μm.

To confirm the presence of specific epithelial subtypes, immunofluorescence staining was performed using Arl13B as a marker for primary cilia and BCAM as a marker for basal cells. Positive staining for both markers confirmed the presence of ciliated and basal cell populations within the ALI cultures (Figure 3). After 2 weeks of culture, tightly packed epithelial cells with a cobblestone-like arrangement and apical microvillar structures were observed by laser scanning confocal microscopy. Nuclear staining with DAPI identified cell nuclei (blue), while abundant Ac-α-tubulin–positive ciliated cells labeled with Alexa Fluor Plus 555 (red) were also detected. These findings were reproducibly observed in all five ALI culture preparations, confirming the validity of this culture system as a differentiation model of human sinonasal epithelium.

 doi:10.20944/preprints202605.1116.v1

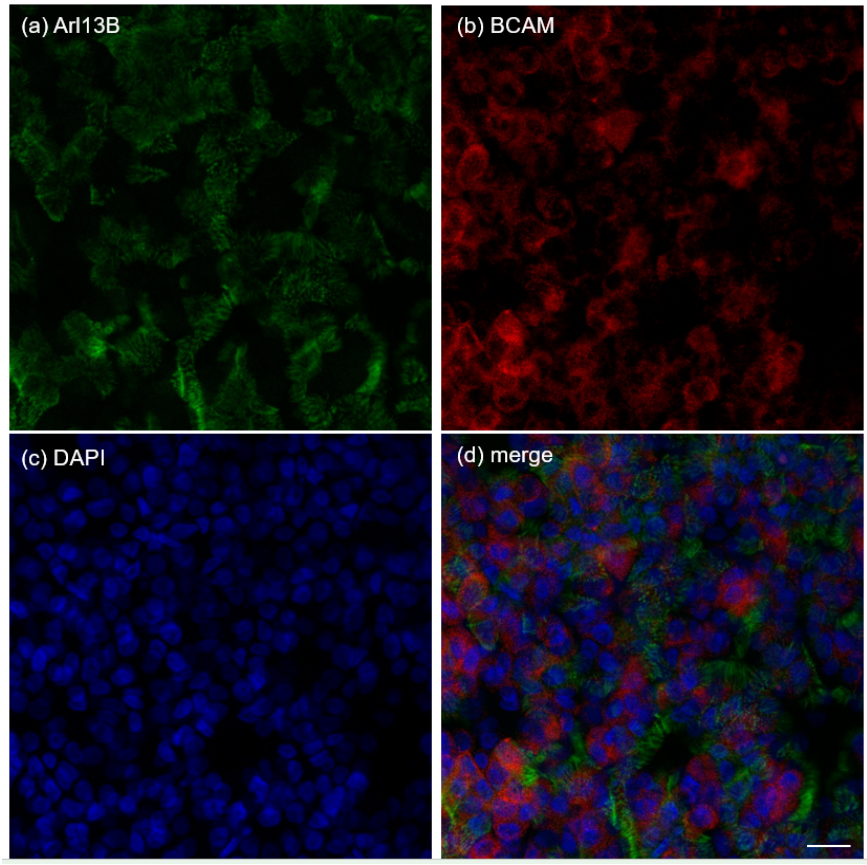

Figure 3. Phenotypic characterization of human sinonasal epithelial cells in ALI culture using cell-specific immunofluorescent markers. (**a–d**) Representative immunofluorescence images of human sinonasal epithelial cells in ALI culture for 4 weeks. Cells show robust expression of Arl13B (green), a marker of primary cilia, and BCAM (red), a marker of basal cells, merged with DAPI (nuclei, blue), confirming development processes to epithelial identity. Scale bars: 15 μm.

3.3. Time-Dependent Changes in Gene Expression During ALI Culture

Temporal changes in gene expression during ALI culture were analyzed by quantitative PCR (qPCR) (Figure 4). Using GAPDH as an internal control, mRNA expression levels of iNOS and BCAM increased significantly over time. In contrast, although eNOS expression showed an increasing trend, the change did not reach statistical significance ($p = 0.131$). These findings suggest that epithelial differentiation during ALI culture is accompanied by enhanced intracellular NO generation mediated through NOS isoforms.

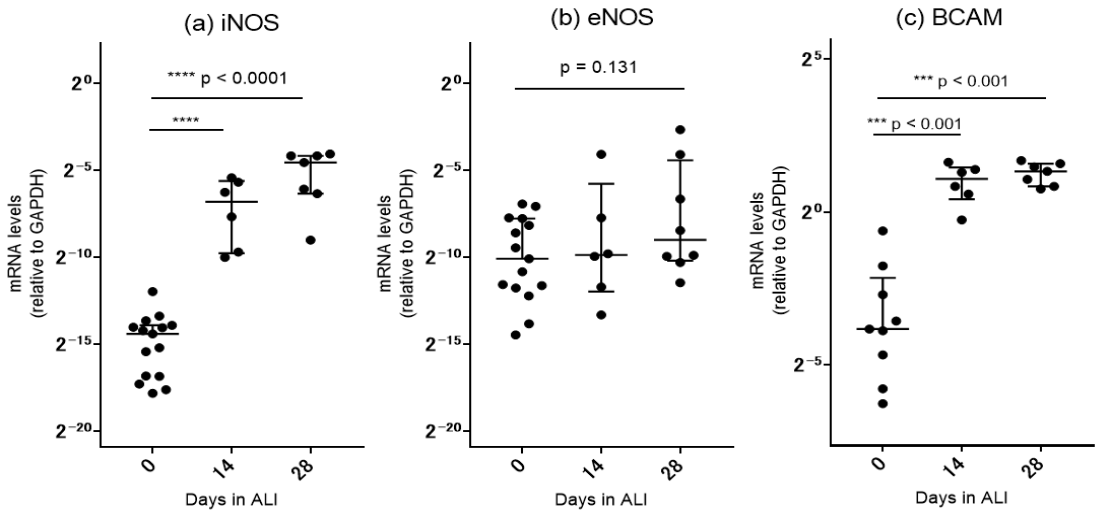

 doi:10.20944/preprints202605.1116.v1

Figure 4. Gene expression of primary sinonasal epithelial cells in ALI cultures. (**a**) iNOS, (**b**) eNOS and (**c**) BCAM mRNA expression increased with 4 weeks of differentiation periods as revealed by qPCR. Data points represent the average of 5 patients.

3.4. Comparison of NO Production Between Epithelial Cell Subtypes

Intracellular NO production in ALI-cultured cells after 4 weeks of differentiation was evaluated using the NO-sensitive fluorescent probe DAF-FM DA (Figure 5). Addition of the NOS substrate L-arginine (0.5 mM) enhanced intracellular green fluorescence intensity, indicating enhanced intracellular NO production. Furthermore, double fluorescence staining with Ac-α-tubulin clearly demonstrated ciliary structures, indicating that ciliated cells were the primary source of NO production.

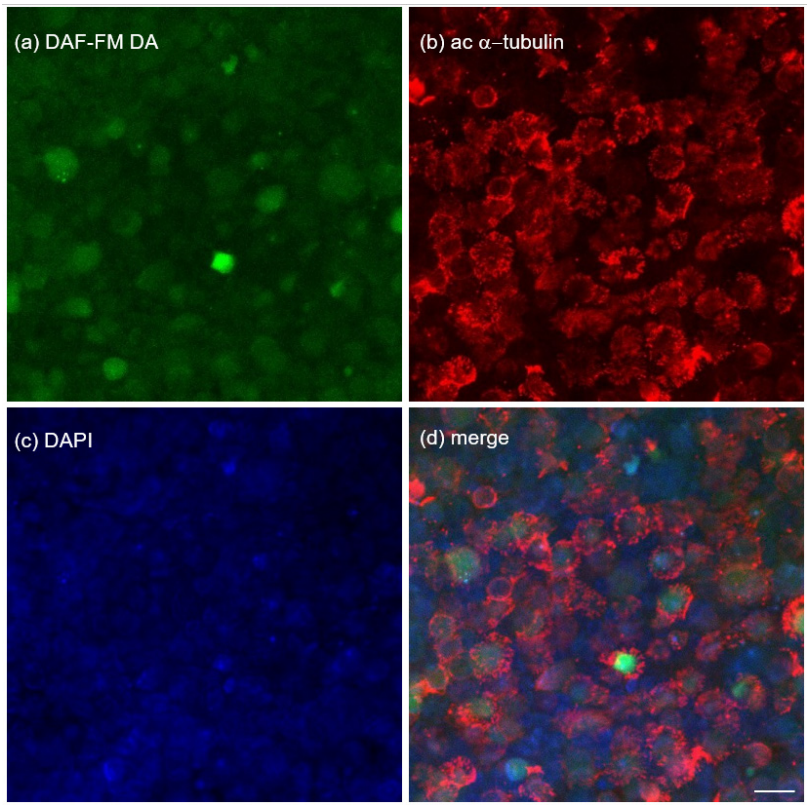

Figure 5. Nitric oxide production in human sinonasal epithelial cells in ALI culture using NO-specific fluorescent indicators DAF-FM DA. Representative LSCM fluorescence images of ALI cultures after 4 weeks of differentiation. (**a**) Cells show distinct NO production as detected by DAF-FM fluorophores (green). (**b**) AlexaFluor 555-labeled staining of ac-tubulin (red) shows abundant apical cilia with a cobblestone epithelial pattern. (**c**) Nuclear DAPI stain is shown in blue. Scale bars: 15 μm.

In the present study, ciliated and non-ciliated epithelial cells differentiated under ALI conditions were identified and compared with respect to NO production capacity. To evaluate the functional contribution of NOS isoforms in each cell type, a non-selective NOS inhibitor (L-NAME) and an iNOS-selective inhibitor (1400W) were used. 1400W is a highly selective inhibitor of iNOS. As shown in Figure 6, marked NO production was observed in ALI-cultured epithelial cells under L-arginine stimulation. DAF-FM fluorescence intensity was markedly higher in ciliated cells (mean 80.3) than in non-ciliated cells (mean 49.3). In contrast, treatment with the non-selective NOS inhibitor L-NAME (0.5 mM for 1 hour) markedly suppressed NO production, reducing fluorescence intensity to 33.4 in ciliated cells and 32.8 in non-ciliated cells, thereby abolishing the difference between the two cell types. Furthermore, although treatment with the iNOS-selective inhibitor 1400W (100 μM)

 doi:10.20944/preprints202605.1116.v1

significantly reduced NO production, fluorescence intensity remained significantly higher in ciliated cells (50.0) than in non-ciliated cells (27.3).

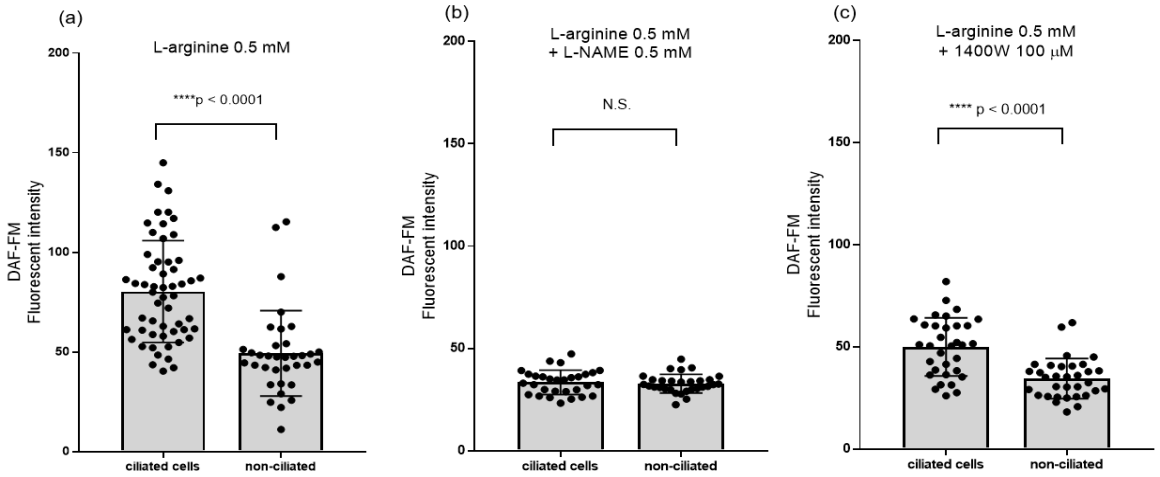

Figure 6. Comparison of nitric oxide (NO) production between ciliated and non-ciliated sinonasal epithelial cells in 4-weeks ALI cultures as revealed by DAF-FM fluorescence. Error bar graphs are combined data from five individual patients. (**a**) Administration of 0.5 mM L-arginine, the NOS substrate, activated NO production. Fully differentiated ciliated cells showed a significant increase in fluorescence intensity as compared with non-ciliated cells. (**b**) Non-specific NOS inhibitor L-NAME (0.5 mM) blocked NO production in both ciliated and non-ciliated cells. There is no difference in DAF-FM fluorescence between the two cell types after L-NAME treatment. (**c**) Pre-treatment with 1400W dihydrochloride, a potent and highly selective inhibitor of iNOS, also resulted in less NO production in both cell types. Ciliated cells showed significantly higher levels of NO production as compared to non-ciliated cells in this condition. *Bar graphs:* mean and SEM. N.S., not significant.

4. Discussion

Chronic rhinosinusitis (CRS) is a persistent inflammatory disease of the nasal cavity and paranasal sinuses characterized by symptoms lasting longer than 12 weeks, including nasal obstruction, purulent rhinorrhea, headache/facial pain, cough, and olfactory dysfunction [1,2]. CRS is not a single disease entity but rather a diagnostic concept encompassing multiple disorders with distinct pathophysiological mechanisms. Currently, CRS is classified phenotypically according to the presence or absence of nasal polyps (CRSwNP vs. CRSsNP), computed tomography (CT) findings, and associated comorbidities such as bronchial asthma (BA) [3–6,29].

Airway cilia play a central role in mucociliary clearance by transporting mucus in a coordinated direction to eliminate pathogens and foreign particles. In CRS, acquired ciliary dysfunction has been suggested, and microscopic studies have demonstrated ciliary loss and disorganized ciliary orientation associated with repeated cycles of infection and inflammation [30]. In addition, sinonasal epithelial cells function not only as a structural barrier but also as “immunologically active cells” that actively regulate immune responses and are considered to play a central role in the formation of type 2 inflammation in CRSwNP [31,32]. Recent single-cell RNA sequencing (scRNA-seq) analyses have demonstrated a reduced proportion of ciliated epithelial cells, abnormal epithelial differentiation, and metabolic dysregulation in CRSwNP [8]. Furthermore, nasal polyp tissues exhibit a decreased epithelial cell population and increased fibroblast infiltration compared with normal mucosa and uncinate process mucosa, suggesting progression of epithelial remodeling [33].

Respiratory ciliated epithelium lining the human paranasal sinuses produces nitric oxide (NO), which contributes to airway defense through antimicrobial activity and enhancement of ciliary motility [11,34]. NO is a highly reactive signaling molecule involved in various physiological and pathological processes, including those in the nervous, vascular, and respiratory systems [10,12–14]. Patients with CRSwNP reportedly exhibit decreased nasal nitric oxide (nNO) levels compared with

 doi:10.20944/preprints202605.1116.v1

healthy controls [11,14,16,17]. In contrast, increased iNOS expression has been observed at the tissue level, suggesting a dissociation between NO production and NO function.

NO is synthesized from L-arginine by nitric oxide synthases (NOS), and three isoforms are present in mammals: nNOS (NOS1), iNOS (NOS2), and eNOS (NOS3) [35,36]. In the sinonasal epithelium, eNOS and iNOS are considered particularly important [11,37]. Under physiological conditions, eNOS primarily generates low concentrations of NO that regulate ciliary motility through the NO–cGMP signaling pathway [12]. In contrast, iNOS is induced by inflammatory stimuli and continuously produces high concentrations of NO, thereby contributing to inflammatory responses. In the present study, increased iNOS expression and an elevated iNOS/eNOS ratio were observed in the CRSwNP group, suggesting qualitative alterations in the NO signaling environment under inflammatory conditions. Thus, NO abnormalities in CRSwNP should not be interpreted simply as reduced NO production, but rather as "dysregulated NO signaling" associated with disruption of the balance among NOS isoforms. Although physiological concentrations of NO enhance ciliary beat frequency (CBF), excessive NO production under inflammatory conditions may instead induce oxidative stress and secondary tissue injury, ultimately leading to ciliary dysfunction [19,38].

Air–liquid interface (ALI) culture is a widely used in vitro technique for establishing stable airway epithelial models that reproduce pseudostratified columnar epithelium containing ciliated cells. This system enables temporal analysis of differentiation from basal cells into ciliated cells, ciliogenesis, and associated changes in functional molecule expression while preserving three-dimensional epithelial architecture. Furthermore, ALI culture reproduces physiological properties of airway epithelium, including mucus secretion and mucociliary transport, making it a valuable model for investigating CRS pathophysiology [39]. In the present study, temporal progression of ALI culture was accompanied by increased expression of iNOS, eNOS, and BCAM, suggesting progressive differentiation toward a ciliated epithelial phenotype. BCAM is recognized as a marker of airway stem/progenitor cells, and its increased expression may reflect maintenance and proliferation of basal cells. On the other hand, BCAM overexpression has also been associated with epithelial differentiation abnormalities and remodeling under inflammatory conditions. Furthermore, sinonasal epithelial cells differentiated under ALI conditions were classified into ciliated and non-ciliated cells, and NO production was compared using DAF-FM fluorescence intensity as an indicator. Consistent with their physiological role, ciliated cells exhibited significantly higher NO production than non-ciliated cells.

DAF-FM DA is an activatable fluorescent probe that emits fluorescence upon reacting with NO. Because it enables conversion of short-lived NO into a stable fluorescent signal, DAF-FM fluorescence has been widely used as an indicator of intracellular NO production [18,24,25]. In vivo fluorescence imaging using DAF-2DA has successfully visualized and quantitatively analyzed NO production in rat mesenteric microcirculation [40]. Moreover, analyses using L-NAME and the NOS1 inhibitor 7-NI demonstrated that NOS1-derived NO predominantly contributes to arteriolar function, whereas NOS3 (eNOS)-derived NO plays a major role in venular function, indicating that the physiological effects of NO are determined by the localization and functional differences among NOS isoforms. The pharmacological characteristics of 1400W, a highly selective iNOS inhibitor, have also been extensively investigated [41]. 1400W exerts potent and time-dependent inhibition against iNOS and exhibits tight binding with slow dissociation, whereas its inhibitory effects on eNOS and nNOS are relatively weak and reversible. Previous studies using murine ischemia–reperfusion models further demonstrated that selective iNOS inhibition by 1400W attenuates tissue injury in the renal cortex, whereas transient endothelial dysregulation may occur in the renal medulla, suggesting that the effects of iNOS inhibition depend on tissue-specific NO signaling balance and endothelial function [42,43].

In the present study, treatment with the non-selective NOS inhibitor L-NAME markedly reduced NO production in ciliated cells, whereas the iNOS-selective inhibitor 1400W did not completely suppress NO production. These findings suggest that NO production in ciliated cells involves multiple NOS isoforms, including both iNOS and eNOS. Importantly, the persistence of NO

 doi:10.20944/preprints202605.1116.v1

production even under iNOS inhibition strongly suggests that constitutive NOS, mainly eNOS, contributes to basal NO production. Regulation of ciliary motility by NO has been reported to occur through the eNOS–NO–sGC–cGMP–PKG pathway [44]. The increase in CBF induced by L-arginine is suppressed by NOS inhibitors, soluble guanylate cyclase (sGC) inhibitors, and PKG inhibitors, supporting the importance of this signaling pathway. The cell type–dependent differences in NOS isoform expression and NO production observed in this study may reflect distinct functional roles in NO signaling. Specifically, physiological NO generated predominantly by eNOS in ciliated cells likely enhances ciliary motility through the cGMP–PKG pathway, whereas inflammatory NO production in non-ciliated cells is primarily iNOS-dependent and contributes less to ciliary motility regulation.

Furthermore, NO-mediated regulation of ciliary motility has been reported to depend on intracellular localization of signaling molecules [45]. Molecules including eNOS, guanylate cyclase (GC), PKG, and PKA localize near the axoneme and basal body. In particular, eNOS, PKG-I, and PKA-RII accumulate around basal bodies, whereas PKA-RI and PKG-II are distributed along the axoneme. Such localization suggests that NO production, cGMP generation, and PKG/PKA activation may function as an integrated localized signaling unit (“metabolon”) near the ciliary apparatus in the vicinity of cilia. In contrast, NO production in non-ciliated cells was almost completely abolished by 1400W, indicating that NO production in these cells is predominantly iNOS-dependent [41]. Because iNOS is induced by inflammatory cytokines and mediates sustained high-output NO production, these findings are consistent with NO production characteristics under inflammatory conditions.

The cell type–dependent differences in NO production observed in the present study are likely closely associated with spatially regulated NO signaling. In ciliated cells, eNOS and iNOS may cooperatively establish a localized NO signaling environment regulating ciliary motility, whereas non-ciliated cells lack such spatial regulation and predominantly generate inflammatory iNOS-derived NO. From this perspective, the reduction of ciliated cells in CRSwNP may represent not merely decreased NO production, but rather a disruption of the spatial regulation of NO signaling. Loss of the local physiological NO signaling environment may impair ciliary motility regulation, resulting in decreased mucociliary clearance and persistence of chronic inflammation. In addition, previous studies have demonstrated reduced nNO levels together with increased iNOS expression and increased proportions of non-ciliated cells in CRSwNP [46–48]. Taken together, these findings suggest that NO signaling may shift from promoting ciliary motility toward amplifying inflammation due to reduced eNOS-derived NO associated with ciliated cell loss and relative increases in inflammation-induced iNOS-derived NO.

Such qualitative alterations in NO signaling are likely involved in impaired mucociliary clearance and persistence of chronic inflammation [49]. These findings support the concept that qualitative dysregulation of NO signaling, rather than simple reductions in NO levels, contributes to epithelial dysfunction and chronic inflammation in CRSwNP. Collectively, ciliary dysfunction and epithelial remodeling in CRSwNP may involve two distinct abnormalities: (1) reduced physiological ciliary regulation mediated by eNOS-dependent NO, and (2) enhanced inflammation and tissue injury mediated by iNOS-dependent NO. Therefore, therapeutic strategies targeting NO signaling should aim not simply at suppressing NO production, but rather at selectively inhibiting iNOS while preserving eNOS function.

Several limitations of this study should be acknowledged. First, this study was based on in vitro analyses using an air–liquid interface (ALI) culture system and therefore does not fully reproduce the in vivo environment. Accordingly, careful interpretation is required regarding the reproducibility of these findings in vivo. Second, it remains unclear whether increased iNOS-derived NO is a primary cause of inflammation or a secondary consequence of inflammatory processes. Additional studies incorporating temporal analyses and in vivo models will be necessary to clarify this issue. Third, the relatively small number of ALI culture preparations may limit the generalizability of the findings. Future studies with larger cohorts are warranted to validate the present results.

 doi:10.20944/preprints202605.1116.v1

5. Conclusions

The present study demonstrated that NO production mechanisms in the sinonasal epithelium differ according to epithelial cell subtype. Both eNOS and iNOS contributed to NO production in ciliated epithelial cells, whereas NO production in non-ciliated epithelial cells was predominantly dependent on iNOS. In CRSwNP, loss of ciliated cells may reduce eNOS-derived physiological NO, while inflammation-induced iNOS-derived NO becomes relatively dominant, thereby shifting NO signaling from physiological regulation of ciliary motility toward inflammatory amplification. These findings provide new insights into the pathophysiology of ciliary dysfunction and epithelial remodeling in CRSwNP and may contribute to the development of novel therapeutic strategies targeting NO signaling.

Author Contributions: Conceptualization, S.H. and S.T.; methodology, S.T., T.S. and T.K.; validation, T.H. and T.U.; formal analysis, S.T., T.K. and T.I.; investigation, S.H., K.K., T.S., R.F., C.I. and Y.H.; resources, S.T. and Y.O.; data curation, S.H., S.T. and T.S.; writing—original draft preparation, S.H.; writing—review and editing, S.T.; visualization, S.H., K.K. and T.S.; supervision, S.T. and T.I.; project administration, S.T.; funding acquisition, S.T. and T.K. All authors have read and agreed to the published version of the manuscript.

Funding: This research was supported by a grant from the Japan Society for the Promotion of Science KAKENHI (no. 25K12743) and a Health Labor Sciences Research grant (no. 24FC1019).

Institutional Review Board Statement: This study was performed in accordance with the Declaration of Helsinki, with approval from the Institutional Review Board at the Hiroshima University School of Medicine (approval no. E2014-9136; approval date: 2 November 2022).

Informed Consent Statement: Written informed consent was obtained from all participants involved in the study.

Data Availability Statement: The data presented in this study are available on reasonable request from the corresponding author.

Acknowledgments: We thank Mr. Kaoru Shingai for technical assistance. We thank the Natural Science Center for Basic Research and Development (N-BARD) for allowing access to scanning electron microscope and laser scanning confocal microscope. The authors are grateful to Yukie Tanaka and Rika Ishikawa for technical instruction of electron microscopy.

Conflicts of Interest: The authors declare no conflicts of interest.

Abbreviations

The following abbreviations are used in this manuscript:

ALI	air–liquid interface
AR	allergic rhinitis
BA	bronchial asthma
BCAM	basal cell adhesion molecule
CBF	ciliary beat frequency
CRS	chronic rhinosinusitis
CRSsNP	chronic rhinosinusitis without nasal polyps
CRSwNP	chronic rhinosinusitis with nasal polyps
DAF-FM DA	4-amino-5-methylamino-2′,7′-difluorofluorescein diacetate
GC	guanylate cyclase
HSNECs	human sinonasal epithelial cells
LSCM	laser scanning confocal microscopy
nNO	nasal nitric oxide
NO	nitric oxide
NOS	nitric oxide synthase
PCP	planar cell polarity

 doi:10.20944/preprints202605.1116.v1

ROI	region of interest
SEM	scanning electron microscopy

References

1. Fokkens, W.J.; Lund, V.J.; Hopkins, C.; Hellings, P.W.; Kern, R.; Reitsma, S.; Toppila-Salmi, S.; Bernal-Sprekelsen, M.; Mullol, J.; Alobid, I.; et al. European position paper on rhinosinusitis and nasal polyps 2020. *Rhinology* **2020**, *58* (Suppl. S29), 1–464. https://doi.org/10.4193/rhin20.600
2. Orlandi, R.R.; Kingdom, T.T.; Smith, T.L.; Bleier, B.; DeConde, A.; Luong, A.U.; Poetker, D.M.; Soler, Z.; Welch, K.C.; Wise, S.K.; et al. International consensus statement on allergy and rhinology: Rhinosinusitis 2021. *Int. Forum Allergy Rhinol.* **2021**, *11*, 213–739. https://doi.org/10.1002/alr.22741
3. Tomassen, P.; Vandeplas, G.; Van Zele, T.; Cardell, L.O.; Arebro, J.; Olze, H.; Förster-Ruhrmann, U.; Kowalski, M.L.; Olszewska-Ziąber, A.; Holtappels, G.; et al. Inflammatory endotypes of chronic rhinosinusitis based on cluster analysis of biomarkers. *J. Allergy Clin. Immunol.* **2016**, *137*, 1449–1456.e4. https://doi.org/10.1016/j.jaci.2015.12.1324
4. Wang, X.; Zhang, N.; Bo, M.; Holtappels, G.; Zheng, M.; Lou, H.; Wang, H.; Zhang, L.; Bachert, C. Diversity of TH cytokine profiles in patients with chronic rhinosinusitis: A multicenter study in Europe, Asia, and Oceania. *J. Allergy Clin. Immunol.* **2016**, *138*, 1344–1353.
5. Bachert, C.; Zhang, N.; Hellings, P.W.; Bousquet, J. Endotype-driven care pathways in patients with chronic rhinosinusitis. *J. Allergy Clin. Immunol.* **2018**, *141*, 1543–1551. https://doi.org/10.1016/j.jaci.2018.03.004
6. Tokunaga, T.; Sakashita, M.; Haruna, T.; Asaka, D.; Takeno, S.; Ikeda, H.; et al. Novel scoring system and algorithm for classifying chronic rhinosinusitis: The JESREC study. *Allergy* **2015**, *70*, 995–1003. https://doi.org/10.1111/all.12644
7. Fujieda, S.; Imoto, Y.; Kato, Y.; Ninomiya, T.; Tokunaga, T.; Tsutsumiuchi, T.; Yoshida, K.; Kidoguchi, M.; Takabayashi, T. Eosinophilic chronic rhinosinusitis. *Allergol. Int.* **2019**, *68*, 403–412. https://doi.org/10.1016/j.alit.2019.07.002
8. Jin, Y.; Liang, Y.; Wang, Z.; Jiang, Y.; Yuan, F.; Zhang, T. Single-cell transcriptomic analysis reveals transcriptome differences of different cells between eosinophilic chronic rhinosinusitis with nasal polyps and non-eosinophilic chronic rhinosinusitis with nasal polyps. *PLoS ONE* **2025**, *20*, e0328241. https://doi.org/10.1371/journal.pone.0328241
9. Wang, Y.; Li, Z.; Lu, J. Single-cell RNA sequencing reveals the epithelial cell, fibroblast, and key gene alterations in chronic rhinosinusitis with nasal polyps. *Sci. Rep.* **2024**, *14*, 2270. https://doi.org/10.1038/s41598-024-52341-8
10. Barnes, P.J. Nitric oxide and airway disease. *Ann. Med.* **1995**, *27*, 389–393. https://doi.org/10.3109/07853899509002592
11. Lundberg, J.; Weitzberg, E.; Rinder, J.; Rudehill, A.; Jansson, O.; Wiklund, N.; Alving, K. Calcium-independent and steroid-resistant nitric oxide synthase activity in human paranasal sinus mucosa. *Eur. Respir. J.* **1996**, *9*, 1344–1347. https://doi.org/10.1183/09031936.96.09071344
12. American Thoracic Society; European Respiratory Society. ATS/ERS recommendations for standardized procedures for the online and offline measurement of exhaled lower respiratory nitric oxide and nasal nitric oxide, 2005. *Am. J. Respir. Crit. Care Med.* **2005**, *171*, 912–930. https://doi.org/10.1164/rccm.200406-710ST
13. Dweik, R.A.; Boggs, P.B.; Erzurum, S.C.; Irvin, C.G.; Leigh, M.W.; Lundberg, J.O.; Olin, A.C.; Plummer, A.L.; Taylor, D.R. An official ATS clinical practice guideline: Interpretation of exhaled nitric oxide levels (FeNO) for clinical applications. *Am. J. Respir. Crit. Care Med.* **2011**, *184*, 602–615. https://doi.org/10.1164/rccm.9120-11ST
14. Barnes, P.J.; Dweik, R.A.; Gelb, A.F.; Gibson, P.; George, S.C.; Grasemann, H.; Pavord, I.D.; Ratjen, F.; Silkoff, P.; Taylor, D.R.; et al. Exhaled nitric oxide in pulmonary diseases: A comprehensive review. *Chest* **2010**, *138*, 682–692. https://doi.org/10.1378/chest.09-2090
15. Jeong, J.H.; Yoo, H.S.; Lee, S.H.; Kim, K.R.; Yoon, H.J.; Kim, S.H. Nasal and exhaled nitric oxide in chronic rhinosinusitis with polyps. *Am. J. Rhinol. Allergy* **2014**, *28*, e11–e16. https://doi.org/10.2500/ajra.2014.28.3984

 doi:10.20944/preprints202605.1116.v1

16. Lee, J.M.; McKnight, C.L.; Aves, T.; Yip, J.; Grewal, A.S.; Gupta, S. Nasal nitric oxide as a marker of sinus mucosal health in patients with nasal polyposis. *Int. Forum Allergy Rhinol.* **2015**, *5*, 894–899. https://doi.org/10.1002/alr.21598
17. Kojima, H.; Nakatsubo, N.; Kikuchi, K.; Kawahara, S.; Kirino, Y.; Nagoshi, H.; Hirata, Y.; Nagano, T. Detection and imaging of nitric oxide with novel fluorescent indicators: Diaminofluoresceins. *Anal. Chem.* **1998**, *70*, 2446–2453.
18. Kuek, L.E.; McMahon, D.B.; Ma, R.Z.; Miller, Z.A.; Jolivert, J.F.; Adappa, N.D.; Palmer, J.N.; Lee, R.J. Cilia stimulatory and antibacterial activities of T2R bitter taste receptor agonist diphenhydramine: Insights into repurposing bitter drugs for nasal infections. *Pharmaceuticals* **2022**, 15, 452. https://doi.org/10.3390/ph15040452
19. Wake, M.; Takeno, S.; Hawke, M. The uncinate process: A histological and morphological study. *Laryngoscope* **1994**, *104*, 364–369. https://doi.org/10.1288/00005537-199403000-00020
20. Takemoto, K.; Lomude, L.S.; Takeno, S.; Kawasumi, T.; Okamoto, Y.; Hamamoto, T.; Ishino, T.; Ando, Y.; Ishikawa, C.; Ueda, T. Functional alteration and differential expression of the bitter taste receptor T2R38 in human paranasal sinus in patients with chronic rhinosinusitis. *Int. J. Mol. Sci.* **2023**, *24*, 4499. https://doi.org/10.3390/ijms24054499
21. Zhan, X.; Li, D.; Johns, R.A. Expression of endothelial nitric oxide synthase in ciliated epithelia of rats. *J. Histochem. Cytochem.* **2003**, *51*, 81–87. https://doi.org/10.1177/002215540305100110
22. Canabal, D.D.; Potian, J.G.; Duran, R.G.; McArdle, J.J.; Routh, V.H. Hyperglycemia impairs glucose and insulin regulation of nitric oxide production in glucose-inhibited neurons in the ventromedial hypothalamus. *Am. J. Physiol. Regul. Integr. Comp. Physiol.* **2007**, *293*, R592–R600. https://doi.org/10.1152/ajpregu.00207.2007
23. Itoh, Y.; Ma, F.H.; Hoshi, H.; Oka, M.; Noda, K.; Ukai, Y.; Kojima, H.; Nagano, T.; Toda, N. Determination and bioimaging method for nitric oxide in biological specimens by diaminofluorescein fluorometry. *Anal. Biochem.* **2000**, *287*, 203–209. https://doi.org/10.1006/abio.2000.4859
24. Tomita, T.; Hirayama, A.; Matsui, H.; Aoyagi, K. Effect of Keishibukuryogan, a Japanese traditional Kampo prescription, on improvement of microcirculation and oketsu and induction of endothelial nitric oxide: A live imaging study. *Evid. Based Complement. Altern. Med.* **2017**, *2017*, 3620130. https://doi.org/10.1155/2017/3620130
25. Takeno, S.; Osada, R.; Furukido, K.; Chen, J.H.; Yajin, K. Increased nitric oxide production in nasal epithelial cells from allergic patients—RT-PCR analysis and direct imaging by a fluorescence indicator: DAF-2 DA. *Clin. Exp. Allergy* **2001**, *31*, 881–888. https://doi.org/10.1046/j.1365-2222.2001.01093.x
26. Berni, M.; Pongolini, S.; Tambassi, M. Automated analysis of intracellular phenotypes of *Salmonella* using ImageJ. *J. Vis. Exp.* **2022**, e64263. https://doi.org/10.3791/64263
27. Ma, Y.; Tian, P.; Zhong, H.; Wu, F.; Zhang, Q.; Liu, X.; Dang, H.; Chen, Q.; Zou, H.; Zheng, Y. WDPCP modulates cilia beating through the MAPK/ERK pathway in chronic rhinosinusitis with nasal polyps. *Front. Cell Dev. Biol.* **2021**, *8*, 630340. https://doi.org/10.3389/fcell.2020.630340
28. Khan, A.; Vandeplas, G.; Huynh, T.; Joish, V.; Mannent, L.; Tomassen, P.; Van Zele, T.; Cardell, L.; Arebro, J.; Olze, H.; et al. The Global Allergy and Asthma European Network (GALEN) rhinosinusitis cohort: A large European cross-sectional study of chronic rhinosinusitis patients with and without nasal polyps. *Rhinology* **2019**, *57*, 32–42. https://doi.org/10.4193/rhin17.255
29. Gudis, D.; Zhao, K.Q.; Cohen, N.A. Acquired cilia dysfunction in chronic rhinosinusitis. *Am. J. Rhinol. Allergy* **2012**, *26*, 1–6. https://doi.org/10.2500/ajra.2012.26.3716
30. Yan, B.; Lan, F.; Li, J.; Wang, C.; Zhang, L. The mucosal concept in chronic rhinosinusitis: Focus on the epithelial barrier. *J. Allergy Clin. Immunol.* **2024**, *153*, 1206–1214. https://doi.org/10.1016/j.jaci.2024.01.015
31. Freund, J.; Mansfield, C.J.; Doghramji, L.J.; Adappa, N.D.; Palmer, J.N.; Kennedy, D.W.; Reed, D.R.; Jiang, P.; Lee, R.J. Activation of airway epithelial bitter taste receptors by *Pseudomonas aeruginosa* quinolones modulates calcium, cyclic-AMP, and nitric oxide signaling. *J. Biol. Chem.* **2018**, *293*, 9824–9840. https://doi.org/10.1074/jbc.RA117.001005

 doi:10.20944/preprints202605.1116.v1

32. Qiu, H.; Liu, J.; Wu, Q.; Ong, H.; Zhang, Y.; Huang, X.; Yuan, T.; Zheng, R.; Deng, H.; Wang, W.; et al. An in vitro study of the impact of IL-17A and IL-22 on ciliogenesis in nasal polyps epithelium via the Hippo-YAP pathway. *J. Allergy Clin. Immunol.* **2024**, *154*, 1180–1194. https://doi.org/10.1016/j.jaci.2024.07.006
33. Guo, F.H.; Erzurum, S.C. Nitric oxide and airway disease. *Environ. Health Perspect.* **1998**, *106* (Suppl. 5), 1119–1124. https://doi.org/10.1289/ehp.98106s51119
34. Alderton, W.K.; Cooper, C.E.; Knowles, R.G. Nitric oxide synthases: Structure, function and inhibition. *Biochem. J.* **2001**, *357*, 593–615. https://doi.org/10.1042/0264-6021:3570593
35. Förstermann, U.; Sessa, W.C. Nitric oxide synthases: Regulation and function. *Eur. Heart J.* **2012**, *33*, 829–837. https://doi.org/10.1093/eurheartj/ehr304
36. Mattila, J.T.; Thomas, A.C. Nitric oxide synthase: Non-canonical expression patterns. *Front. Immunol.* **2014**, *5*, 478. https://doi.org/10.3389/fimmu.2014.00478
37. Kawasumi, T.; Takeno, S.; Ishikawa, C.; Takahara, D.; Taruya, T.; Takemoto, K.; Hamamoto, T.; Ishino, T.; Ueda, T. The Functional Diversity of Nitric Oxide Synthase Isoforms in Human Nose and Paranasal Sinuses: Contrasting Pathophysiological Aspects in Nasal Allergy and Chronic Rhinosinusitis. *Int. J. Mol. Sci.* **2021**, *22*, 7561. https://doi.org/10.3390/ijms22147561
38. Lee, R.E.; Reidel, B.; Nelson, M.R.; Macdonald, J.K.; Kesimer, M.; Randell, S.H. Air–liquid interface cultures to model drug delivery through the mucociliary epithelial barrier. *Adv. Drug Deliv. Rev.* **2023**, *198*, 114866. https://doi.org/10.1016/j.addr.2023.114866
39. Kashiwagi, S.; Kajimura, M.; Yoshimura, Y.; Suematsu, M. Nonendothelial source of nitric oxide in arterioles but not in venules: Alternative source revealed in vivo by diaminofluorescein microfluorography. *Circ. Res.* **2002**, *91*, e55–e64. https://doi.org/10.1161/01.RES.0000047529.26278.4D
40. Garvey, E.P.; Oplinger, J.A.; Furfine, E.S.; Kiff, R.J.; Laszlo, F.; Whittle, B.J.; Knowles, R.G. 1400W is a slow, tight-binding, and highly selective inhibitor of inducible nitric-oxide synthase in vitro and in vivo. *J. Biol. Chem.* **1997**, *272*, 4959–4963. https://doi.org/10.1074/jbc.272.8.4959
41. Pasten, C.; Lozano, M.; Méndez, G.P.; Irarrázabal, C.E. 1400W prevents renal injury in the renal cortex but not in the medulla in a murine model of ischemia and reperfusion injury. *Cell Physiol. Biochem.* **2022**, *56*, 573–586. https://doi.org/10.33594/000000577
42. Pasten, C.; Lozano, M.; Osorio, L.A.; Cisterna, M.; Jara, V.; Sepúlveda, C.; Ramírez-Balaguera, D.; Moreno-Hidalgo, V.; Arévalo-Gil, D.; Soto, P.; et al. The protective effect of 1400W against ischaemia and reperfusion injury is countered by transient medullary kidney endothelial dysregulation. *J. Physiol.* **2024**, in press. https://doi.org/10.1113/JP285944
43. Jiao, J.; Wang, H.; Lou, W.; Jin, S.; Fan, E.; Li, Y.; Han, D.; Zhang, L. Regulation of ciliary beat frequency by the nitric oxide signaling pathway in mouse nasal and tracheal epithelial cells. *Exp. Cell Res.* **2011**, *317*, 2548–2553. https://doi.org/10.1016/j.yexcr.2011.07.007
44. Stout, S.L.; Wyatt, T.A.; Adams, J.J.; Sisson, J.H. Nitric oxide-dependent cilia regulatory enzyme localization in bovine bronchial epithelial cells. *J. Histochem. Cytochem.* **2007**, *55*, 433–442. https://doi.org/10.1369/jhc.6A7089.2007
45. Takeno, S.; Taruya, T.; Ueda, T.; Noda, N.; Hirakawa, K. Increased exhaled nitric oxide and its oxidation metabolism in eosinophilic chronic rhinosinusitis. *Auris Nasus Larynx* **2013**, *40*, 458–464. https://doi.org/10.1016/j.anl.2013.02.001
46. Deja, M.; Busch, T.; Bachmann, S.; Riskowski, K.; Campean, V.; Wiedmann, B.; Schwabe, M.; Hell, B.; Pfeilschifter, J.; Falke, K.J.; et al. Reduced nitric oxide in sinus epithelium of patients with radiologic maxillary sinusitis and sepsis. *Am. J. Respir. Crit. Care Med.* **2003**, *168*, 281–286. https://doi.org/10.1164/rccm.200207-640OC

 doi:10.20944/preprints202605.1116.v1

47. Tang, B.; Tu, J.; Zhang, M.; Zhang, Z.; Yu, J.; Shen, L.; Luo, Q.; Ye, J. Diagnostic value and underlying mechanism of nasal nitric oxide in eosinophilic chronic rhinosinusitis with nasal polyps. *Mol. Immunol.* **2023**, *159*, 1–14. https://doi.org/10.1016/j.molimm.2023.05.004
48. Hirokane, S.; Kawasumi, T.; Takeno, S.; Okamoto, Y.; Miyamoto, S.; Fujita, R.; Ishikawa, C.; Oda, T.; Horibe, Y.; Ishino, T.; et al. Impaired coordination of the ciliary movement in patients with chronic rhinosinusitis with nasal polyps: The role of decreased planar cell polarity protein expression. *Immuno* **2024**, *4*, 247–265. https://doi.org/10.3390/immuno4030016